Biological Psychiatry

Archival Report

Spatial Dynamic Subspaces Encode Sex-Specific Schizophrenia Disruptions in Transient Network Overlap and Their Links to Genetic Risk

Armin Iraji, Jiayu Chen, Noah Lewis, Ashkan Faghiri, Zening Fu, Oktay Agcaoglu, Peter Kochunov, Bhim M. Adhikari, Daniel H. Mathalon, Godfrey D. Pearlson, Fabio Macciardi, Adrian Preda, Theo G.M. van Erp, Juan R. Bustillo, Covadonga M. Díaz-Caneja, Pablo Andrés-Camazón, Mukesh Dhamala, Tulay Adali, and Vince D. Calhoun

ABSTRACT

BACKGROUND: Schizophrenia research reveals sex differences in incidence, symptoms, genetic risk factors, and brain function. However, a knowledge gap remains regarding sex-specific schizophrenia alterations in brain function. Schizophrenia is considered a dysconnectivity syndrome, but the dynamic integration and segregation of brain networks are poorly understood. Recent advances in resting-state functional magnetic resonance imaging allow us to study spatial dynamics, the phenomenon of brain networks spatially evolving over time. Nevertheless, estimating time-resolved networks remains challenging due to low signal-to-noise ratio, limited short-time information, and uncertain network identification.

METHODS: We adapted a reference-informed network estimation technique to capture time-resolved networks and their dynamic spatial integration and segregation for 193 individuals with schizophrenia and 315 control participants. We focused on time-resolved spatial functional network connectivity, an estimate of network spatial coupling, to study sex-specific alterations in schizophrenia and their links to genomic data.

RESULTS: Our findings are consistent with the dysconnectivity and neurodevelopment hypotheses and with the cerebello-thalamo-cortical, triple-network, and frontoparietal dysconnectivity models, helping to unify them. The potential unification offers a new understanding of the underlying mechanisms. Notably, the posterior default mode/salience spatial functional network connectivity exhibits sex-specific schizophrenia alteration during the state with the highest global network integration and is correlated with genetic risk for schizophrenia. This dysfunction is reflected in regions with weak functional connectivity to corresponding networks.

CONCLUSIONS: Our method can effectively capture spatially dynamic networks, detect nuanced schizophrenia effects including sex-specific ones, and reveal the intricate relationship of dynamic information to genomic data. The results also underscore the clinical potential of dynamic spatial dependence and weak connectivity.

https://doi.org/10.1016/j.biopsych.2023.12.002

Schizophrenia is a complex neuropsychiatric disorder that significantly burdens society (1) and presents a wide array of symptoms, including hallucinations, delusions, disorganized speech and behavior, and cognitive impairments (2,3). Understanding the underlying neurobiological mechanisms of schizophrenia is imperative for developing effective interventions and treatments, with sex being an important factor influencing outcomes and strategies. Notably, research has elucidated sex/gender differences in the incidence and clinical manifestation of mental disorders (4,5). Females with schizophrenia tend to exhibit more depressive symptoms, whereas males often experience more negative symptoms (6,7). Sex differences have also been identified in cognitive tasks (8), genetics (9), and neurobiology (8,10). Previous findings support the notion that autosomal genes interact with sex to influence the risk for schizophrenia (9,11–13). Moreover, polygenic risk scores for schizophrenia are negatively correlated with cognitive performance in males exclusively (14). However, a substantial knowledge gap remains regarding sex-specific schizophrenia alterations in brain function and their link to schizophrenia genetic risk factors.

At the brain level, schizophrenia is hypothesized as a disconnection syndrome, where disruptions in functional integrations have a greater influence on behavior and psychopathology than aberrations in single brain regions (15,16). Thus, extensive efforts have been directed toward identifying these disruptions using resting-state functional magnetic resonance imaging (rsfMRI) to unravel the underlying neurobiology of schizophrenia (17–25). Recent research also shows sex differences in functional connectivity aberrations in

© 2023 Society of Biological Psychiatry. This is an open access article under the CC BY-NC-ND license (http://creativecommons.org/licenses/by-nc-nd/4.0/).

ISSN: 0006-3223

schizophrenia (20). The default mode network (DMN) and salience network (SN) have been associated with negative symptoms, which are more pronounced in men with schizophrenia (6,8,19,26–28). Their functional connectivity mediates the link between sex and mental rotation (29), potentially explaining schizophrenia-by-sex interactions in the mental rotation task (8). Sex differences in functional connectivity were observed in autism spectrum disorder (30), which shares significant clinical and genetic components with schizophrenia (31).

Nonetheless, research is lacking on how brain functional units spatially integrate and segregate over time in schizophrenia and how sex-specific schizophrenia differences in brain function are related to genetic risk factors.

Spatially Dynamic Analyses in rsfMRI: Quantifying Spatial Network Coupling

The brain maintains, regulates, adapts, and responds to a rich repertoire of behavior and mental activities via the continuous reconfiguration of coordinated intrinsic activities. On a large scale, these activities are thought to manifest as a set of discrete yet interactive neuronal assemblies, commonly referred to as functional units or functional sources (32). This view has gained traction in the field of rsfMRI, where spatially fixed nodes or data-driven estimations of functional sources, e.g., functional networks (33–35) or functional parcels (36–38), have been used to model the functional interactions among functional sources. Studies often assume that functional sources remain spatially fixed throughout the scan and use average voxel time series from fixed spatial regions to estimate sources' time courses and compute whole-brain static or temporally dynamic functional connectivity. However, the continuous reconfiguration of coordinated intrinsic activities can result in changes in the spatial patterns of functional units over time (i.e., spatial dynamics) (22,32,39–41). Consequently, relying solely on the average time series over anatomically fixed regions, which overlooks spatial dynamics, leads to suboptimal functional connectivity estimation and imprecise inferences.

In addition, spatial dynamics carry unique information hidden from existing spatially static approaches, particularly regarding the spatial coupling and uncoupling of functional units over time. Our previous work (39) has shown that brain networks can dynamically segregate and integrate in space, including the transient emergence of the cerebellar and primary visual networks within the spatial patterns of other brain networks.

Here, we leveraged spatial dependence to quantify dynamic integration and segregation in brain networks, thereby enhancing our understanding of the dynamic interplay between integrative and specialized processes. We use the term spatial functional network connectivity (spFNC) to describe the spatial dependence between networks, consistent with the definition of temporal FNC, which refers to the temporal dependence between networks.

METHODS AND MATERIALS

Dataset and Preprocessing

We analyzed multicenter 3T rsfMRI data (18,42,43). Quality control and preprocessing followed the NeuroMark protocol (34). The inclusion criteria were 1) minimum of 100 volumes for rsfMRI data (all data exceeded 140 volumes), 2) head motion within 3° rotations and 3-mm translations in each direction, 3) mean framewise displacement (44) < 0.25, 4) accurate registration to the template, and 5) spatial overlap exceeding 80% between individual and group masks. This resulted in a sample comprising 193 participants with schizophrenia and 315 matched control participants (Table 1). Preprocessing steps included excluding the first 5 volumes, slice-timing and rigid body motion corrections, registration to a Montreal Neurological Institute template, resampling to 3 mm^3 isotropic voxels, and spatial smoothing with a 6-mm full width at half maximum Gaussian kernel. Additionally, voxel time courses were detrended, despiked, motion corrected, and filtered to reduce noise and nuisance signals (39). See the Supplement for details regarding dataset, recruitment strategies, inclusion/exclusion criteria, demographic variables, and preprocessing.

RESULTS

Capturing Time-Resolved Network-Specific Spatial Patterns

To effectively estimate time-resolved spFNCs, we introduced a time-resolved, reference-informed network estimation approach that derived time-varying spatial maps for each network while controlling for the impact of other networks, thereby disentangling their specific contributions over time (Figure 1). This approach also overcomes the uncertainty of post hoc matching, which can be more problematic in a time-resolved setting (35,45). Furthermore, the combination of reference-informed and spatial-constraint mechanisms effectively addresses the challenges of low signal-to-noise ratio and limited information in short time segments. Spatial constraints restrict the search space and act as regularizers, mitigating overfitting to noise and enabling the capture of the underlying signal.

First, we performed group-level spatial independent component analysis (ICA) (46) with a model order of 20 (39,47) using the Group ICA of FMRI Toolbox (http://trendscenter.org/software/gift) and obtained large-scale brain networks used as the templates for downstream analysis (Figure 1A). Fourteen components of 20 with very high ICASSO stability indexes (average ± SD = 0.96 ± 0.01, minimum–maximum = 0.93–0.98) were identified as brain networks based on their temporal and spatial properties and knowledge from previous studies (35,39,47). These include the primary and secondary visual (VIS-P/VIS-S), primary and secondary somatomotor (MTR-P/

Table 1. Demographic Information

	Sex, Female/Male	Age, Years	Population, Ancestry, Descent, or Nationality, AMR/EUR/O[a]
Control Group, $n = 315$	130/185	38.40 ± 12.73	65/192/58
Schizophrenia Group, $n = 193$	39/154	38.61 ± 13.29	44/112/37

Values are presented as n or mean ± SD.

AMR, American ancestry; EUR, European ancestry; O, Other (African American ancestry or East Asian ancestry).

[a]Based on 1000 Genomes Project superpopulations.

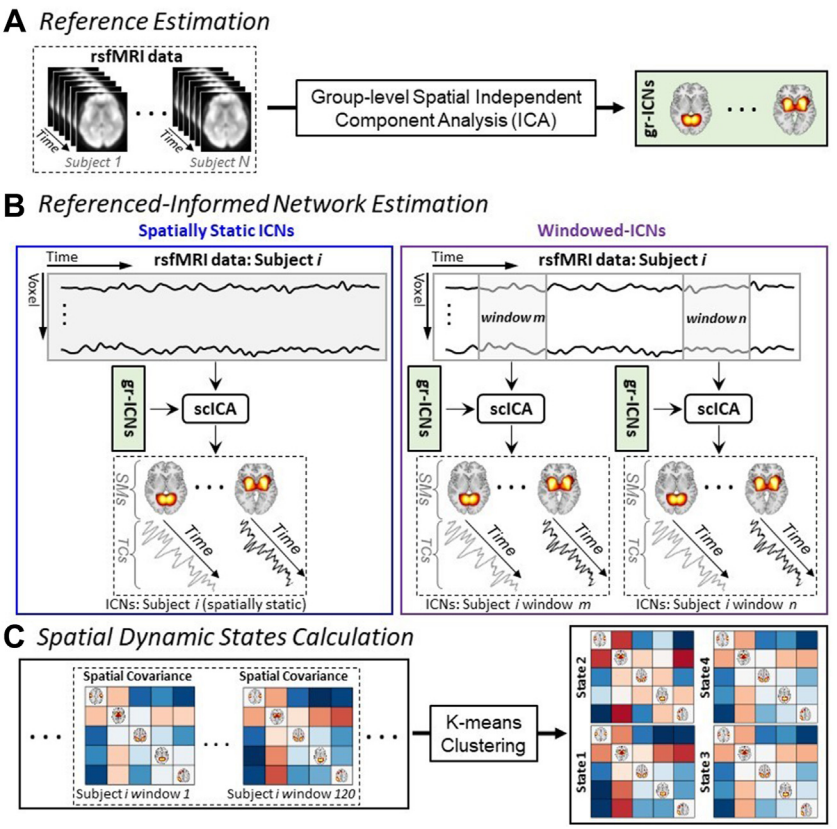

Figure 1. Schematic of the analysis pipeline. **(A)** Using group-level spatial independent component analysis (ICA) to obtain group-level intrinsic connectivity networks as a functional unit reference. **(B)** Applying spatially constrained ICA (scICA) to estimate the correspondence of intrinsic connectivity networks (ICNs) from a given participant. The left panel shows the standard scICA application to estimate spatially static ICNs (i.e., assume spatial patterns of ICNs remained fixed over time), and the right panel shows the proposed approach to estimate time-resolved ICN information. **(C)** Calculating whole-brain spatial dynamic states from spatial covariance matrices. gr-ICN, group-level ICN; rsfMRI, resting-state functional magnetic resonance imaging; SMs: spatial maps; TCs: time courses.

MTR-S), subcortical (SUB), cerebellar (CER), attention (ATN), frontal (FRNT), left and right frontoparietal (FPN-L/FPN-R), posterior and anterior default mode (DMN-P/DMN-A), salience (SN), and temporal (TEMP) networks (Figure 2A). Moreover, separate ICAs conducted for each sex group identified similar networks for men and women with high spatial similarity (0.92 ± 0.05 and 0.92 ± 0.03, respectively).

Next, we combined a spatially constrained ICA method called multivariate-objective optimization ICA with reference (48) (Figure 1B, left) and the sliding window technique (49) to estimate time-resolved networks corresponding to the templates (Figure 1B, right). This ICA approach performs well in capturing sample-specific information for different data lengths and brain networks (35) and is robust to artifacts (50). The sliding window technique is the most commonly used technique to study brain dynamics due to its simplicity, ease of use, and similarity to the conventional functional connectivity procedure, making the interpretation of findings straightforward (49). We used a tapered window (rectangle width = 60 seconds, Gaussian σ = 6 seconds) with a sliding step size of 1, consistent with previous recommendations (49,51) and our previous research in spatial dynamics (39), ensuring consistency and comparability of findings across studies.

Low-Dimensional Spatial Dynamic States Encapsulates Global Brain State Dynamics

We quantified time-resolved spFNCs by calculating spatial covariance of networks at each time window, where an increase and decrease indicate network integration and segregation. Next, we captured global brain state dynamics by identifying 4 recurring, distinct spFNC patterns (Figure 2C) using *k*-means clustering with L1 distance and the elbow criterion (Figure 2B), following previous work and recommendations (20,49,52).

The fraction of time that individuals spent in spatial dynamics states varied significantly, with state 4 having an approximately 2-fold higher fraction rate than state 2 (0.31 vs. 0.17). State 4 demonstrated the lowest level of overall network integration, while states 1 and 2 showed the highest integration. Conversely, the mean dwell time, which indicates the amount of time spent at each state per visit, was very similar across all states, ranging from 18.95 to 22.03 seconds. In other words, while the life expectancy of spatial dynamic states (i.e., mean dwell time) is similar on average, the total amount of time the brain stays in each state varies.

The Clinical Relevance of Dynamic Spatial Coupling: A Schizophrenia Study

Next, we investigated alterations in the continuous reconfiguration of functional integration and segregation in schizophrenia. Given the previous findings (17–20,23,24,26,39), we hypothesized alterations in the dynamic spFNC of large-scale networks in schizophrenia, including sex-specific disruptions in the posterior DMN (pDMN)/SN spFNC.

We ran a generalized linear regression model for each spFNC pair from each spatial dynamic state with age, sex,

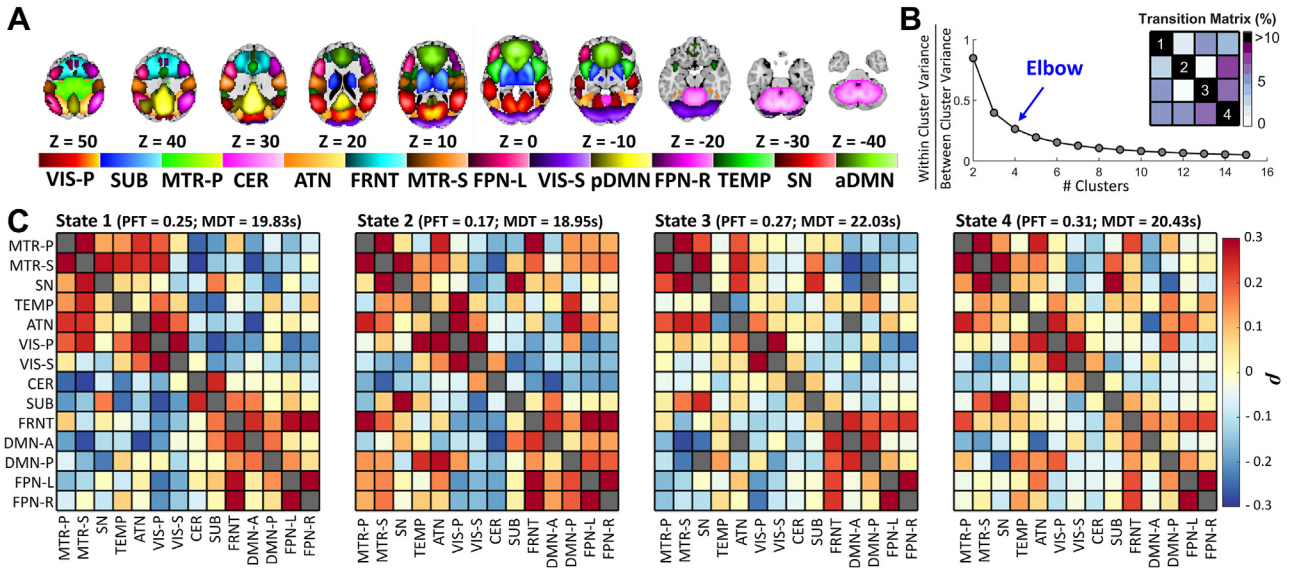

Figure 2. Capturing global brain state dynamics using low-dimensional spatial dynamic states. **(A)** Visualization of the intrinsic connectivity networks. Each color in the composite map represents the spatial map of 1 intrinsic connectivity network thresholded at $|Z| > 1.96$ ($p = .05$). **(B)** Estimation of the optimal number of states. The *k*-means clustering procedure was conducted for cluster numbers 1 to 15. The ratio of within- to between-cluster variance was calculated for each clustering, and the elbow criterion was used to estimate the number of global states. **(C)** The 4 spatial dynamic states were identified using *k*-means clustering with L1 distance. The fraction rate is the fraction of times a participant spends in a given state, and mean dwell time represents the average time a given participant stays in a given state before switching to another state. The mean dwell time is similar across states (18.95 ∼ 22.03 seconds), while fraction rate shows more difference across states (0.17 ∼ 0.31). aDMN, anterior default mode network; ATN, attention network; CER, cerebellar network; FPN, frontoparietal network; FRNT, frontal network; L, left; MDT, mean dwell time; MTR, somatomotor network; P, primary; pDMN, posterior default mode network; PFT, percentage fraction rate; R, right; S, secondary; SN, salience network; SUB, subcortical network; TEMP, temporal network; VIS, visual network.

mean framewise displacement, and site as confounding factors and diagnosis and sex-by-diagnosis interactions as predictors of interest. The *p* values were corrected using a 5% false discovery rate (53).

We observed system-wide disruptions in dynamic functional integration (Figure 3), among which the spFNC pairs of the CER, TEMP, and MTR-S were affected the most. As hypothesized, the dynamic spatial coupling between the pDMN and SN revealed sex-specific changes in schizophrenia. The sex-specific effect also existed in dynamic spFNC network pairs of CER/MTR-S and SUB/FRNT. The sex-specific effect of schizophrenia was only significant in state 1, the state with the highest level of system-wide functional integration.

Next, we evaluated the genomic predisposition of aberrant system-wide dynamic functional integration. We focused on the schizophrenia-risk single nucleotide polymorphisms that reside in the 287 loci reported by a recent large-scale schizophrenia genomic study (54) and computed the polygenic risk score for schizophrenia pruned at $R^2 < 0.1$ (54) using PRSice (55). Sixteen of the annotated genes have been implicated for credible causal nonsynonymous or untranslated region variation, and the enrichment test has pointed to postsynaptic pathology (54). Details regarding these 287 risk loci are available in Supplementary Table 3 of Trubetskoy *et al.* (54). The associations between the polygenic risk score and aberrant dynamic spFNC were performed on a subset of data (European/American = 304/109, schizophrenia/control = 156/257) using Pearson correlations while controlling for diagnosis, sex, age, mean framewise displacement, and site and correcting for multiple comparisons using the false discovery rate. Two dynamic spFNC pairs exhibited significant correlations with the polygenic risk score for schizophrenia, including pDMN/SN spFNC in state 1 with a sex-specific schizophrenia effect and TEMP/MTR-P spFNC in state 2 with a significant diagnosis effect (Figure 3C). We also investigated these associations separately in European and American populations and observed consistent associations with comparable effect sizes.

Low Regional Contribution Linked to High Informational Content

Next, we investigated how schizophrenia-related alterations in low-dimensional spatial dynamic states were linked to diagnosis differences in high-dimensional voxel space by focusing on the dynamic spFNC pairs with both significant schizophrenia effects and genomic associations. Voxelwise statistical comparisons were conducted on the networks' state spatial maps using the same regression model as for spFNC analysis, which resulted in 1 spatial map of beta coefficients for each variable of interest. Subsequently, we computed the spatial similarity between each beta-spatial map and the spatial maps of networks involved in each spFNC pair using Pearson correlations and compared it with the spatial similarity estimated from null data with the same level of spatial smoothing.

Our results suggest that 1) the aberrations of brain networks reflect changes in dynamic spFNC; 2) schizophrenia affects brain networks in a nuanced and distributed manner across the entire brain; 3) regions with lower network contributions

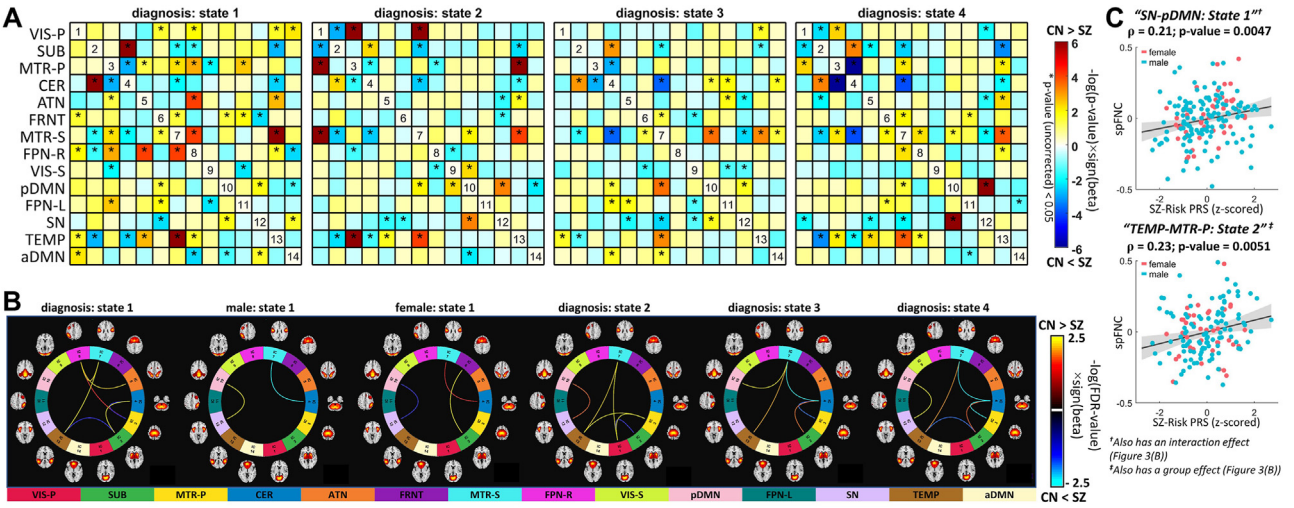

Figure 3. Global spatial dynamic disruption in schizophrenia (SZ) and association with genomic data. **(A)** The diagnosis effect (before correcting for multiple comparisons), i.e., SZ vs. control (CN), of the identified spatial functional network connectivity (spFNC) dynamic states. The statistical comparison for each per-state spFNC pair was conducted using a generalized linear regression model with age, sex, mean framewise displacement, and site as confounding factors and diagnosis and sex-by-diagnosis interactions as predictors of interest. Asterisks (*) represent $p < .05$. **(B)** Connectograms of state spFNC pairs with a significant diagnosis or interaction (diagnosis-by-sex) effects after false discovery rate corrections. Three spFNC pairs from state 1 show significant sex-by-diagnosis interaction effects, including the posterior default mode network (pDMN) and salience network (SN). **(C)** The association between SZ genetic risk and aberrant dynamic spatial coupling. Among dynamic spFNC pairs with a significant SZ effect, 2 show significant associations with the polygenic risk score (PRS) after false discovery rate correction. These 2 include the spFNC between the pDMN and SN in state 1 with a sex-specific SZ effect and the spFNC between the temporal network (TEMP) and primary somatomotor network (MTR-P) in state 2, which show disruption in SZ but with no significant sex effect. aDMN, anterior default mode network; ATN, attention network; CER, cerebellar network; FPN, frontoparietal network; FRNT, frontal network; L, left; P, primary; R, right; S, secondary; SUB, subcortical network; VIS, visual network.

demonstrate a more prominent effect; and 4) the impact of schizophrenia may not necessarily be strongly evident for single voxels despite significant whole-brain effects.

Figure 4A shows the spatial similarity between the beta-spatial maps of variables of interest (e.g., diagnosis) and the network maps, with significant similarities indicated by asterisks. Figure 4B shows the beta-spatial maps with significant spatial similarity. The beta-spatial map of SN state 1 for the sex-by-diagnosis interaction and male diagnosis effects (but not for the group diagnosis effect) showed significant spatial similarities with the pDMN (Figure 4A). Similarly, the beta-spatial maps of the interaction (sex-by-diagnosis) and diagnosis (male) effects for the state 1 pDMN had significant similarities with the spatial map of the SN (Figure 4A). These findings bolster the sex-specific schizophrenia effect observed in pDMN/SN spFNC in state 1 (Figure 3).

For the state 1 pDMN, the impact of schizophrenia was not strong enough to manifest at the voxel level (Figure 4C) despite the significant global effect. However, the SN map in state 1 revealed significant interaction and male diagnosis effects in regions commonly associated with the pDMN, including the posterior cingulate cortex and precuneus (Figure 4C). These regions with notable sex-specific schizophrenia effects have often been masked out in previous research due to their weak functional connectivity to their respective networks.

For the MTR-P and TEMP in state 2 with significant diagnostic effects in their spFNC (Figure 3), the beta-spatial map of the diagnosis effect showed significant spatial similarity with the TEMP and MTR-P, respectively (Figure 4A). At the voxel level, regions with significant diagnosis group effects for the TEMP resembled the MTR-P (Figure 4C). For the MTR-P, the diagnosis group effect spatial map contains a brain area with a significant contribution to the TEMP but also contains regions of the primary visual network, which also showed aberrant FNC with the MTR-P in state 2.

We also conducted a voxelwise analysis to evaluate the associations between the polygenic risk score and state network spatial maps. We found significant spatial similarities ($p < .05$) between the genomic association maps and all 4 networks' state spatial maps. For example, the genomic association map for the state 1 pDMN showed significant spatial similarity with the SN map ($p = .03$).

DISCUSSION

Our research aims to explore the potential benefits of dynamic spatial integration and segregation of brain networks in the context of schizophrenia, with a particular focus on sex-specific alterations and their links to genetic risk factors.

To achieve this goal and address existing challenges, we have introduced a reference-informed network estimation technique that effectively estimates time-resolved networks from short time segments while also controlling for the influence of other networks in the estimations. This has a potential advantage over our previous work (39), which utilized sliding window correlation as an alternative approach. Furthermore, compared to our previous effort (56), this method is more generalizable, computationally efficient, and capable of capturing information about the second- and higher-order statistics of spatial dependence. This allows us to more

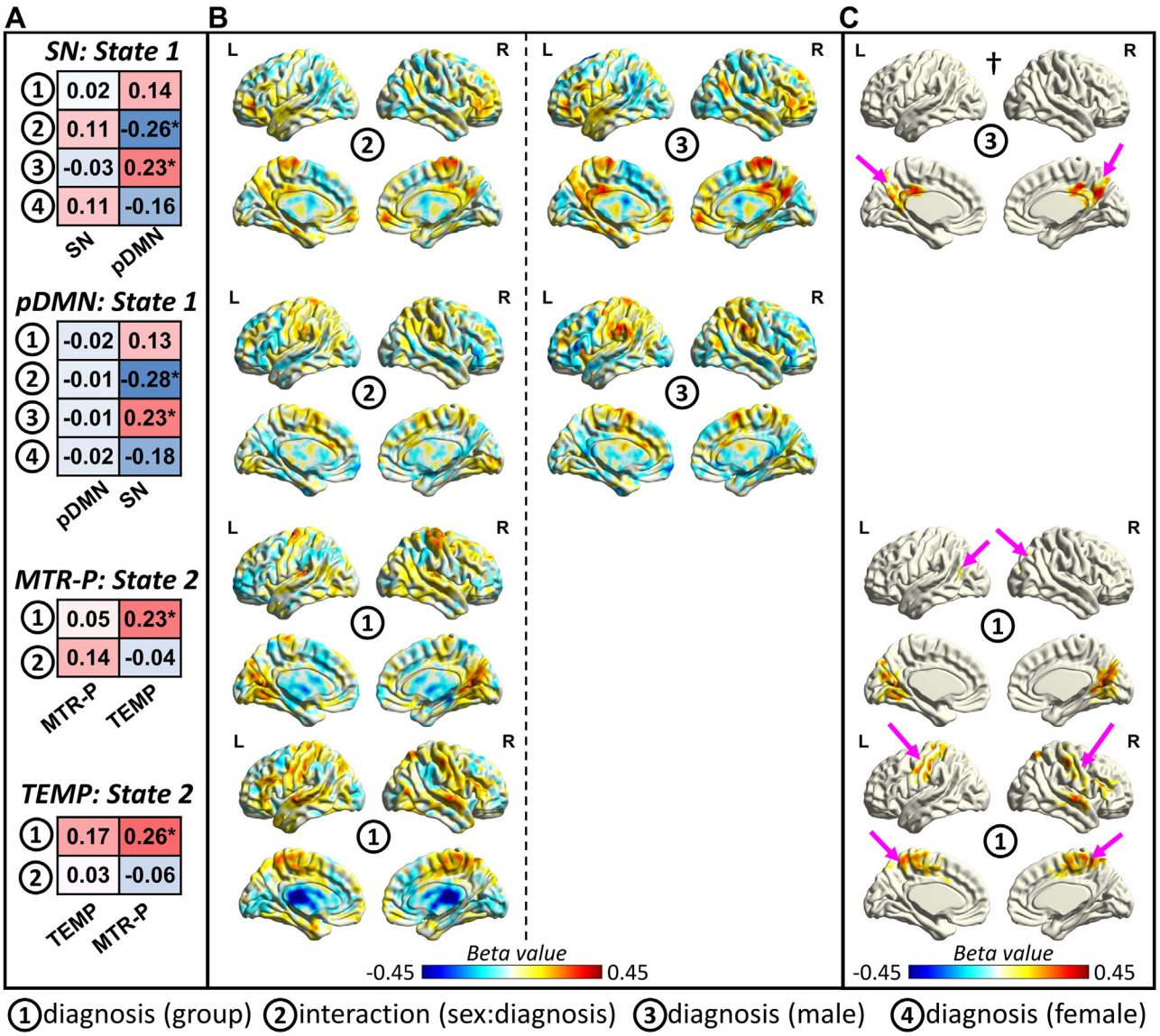

Figure 4. The evidence of aberrant dynamic spatial coupling on network dynamic spatial maps. We conducted voxelwise statistical analysis on the spatial patterns of the networks to evaluate whether the effect of schizophrenia on dynamic spatial functional network connectivity emerges in the network dynamic spatial maps. We focused on the spatial patterns involved in the 2 spatial functional network connectivity pairs with significant schizophrenia effects and genomic associations. **(A)** The results of the spatial similarity (measured by Pearson correlation) between the spatial map of a specific network for a given state and the beta-spatial maps of the variables of interest (e.g., diagnosis) from voxelwise statistical analysis. Asterisks represent those with significant spatial similarity (p value $< .05$), and the value in each cell represents the Pearson correlation coefficient. The results are consistent with dynamic spatial functional network connectivity findings. For example, we observe significant spatial similarity with the posterior default mode network (pDMN) for the interaction effect in the salience network (SN) state 1. Another example is the spatial map of the diagnosis group effect (but not the interaction effect) obtained using voxelwise analysis of the primary somatomotor network (MTR-P) in state 2, which shows significant spatial similarity with the spatial map of the temporal network (TEMP). **(B)** The beta-spatial maps of those that show significant spatial similarity in **(A)**. To study the impact of schizophrenia at the voxel level, cluster-wise correction was applied to beta-spatial maps. **(C)** Cluster-corrected statistics. Pink arrows illustrate clusters in which the paired networks have a strong contribution. For example, the pink arrows in † show the cluster in the posterior cingulate cortex and precuneus that survived cluster-wise correction. The posterior cingulate cortex and precuneus are the cores of the pDMN and contribute significantly to the pDMN. L, left; R, right.

accurately quantify dynamic integration and segregation, thereby enhancing our understanding of dysconnectivity in brain dynamics associated with schizophrenia.

We identified 4 distinct spatial dynamic states with unique network integration and segregation patterns, which collectively provide a low-dimensional summary of global brain state dynamics. The brain spends more time in state 4, the most segregated state with the highest rate of between-state transitioning. We propose that this state functions as a hub-like transition state. However, all states have a similar life

expectancy, suggesting that state 4 is not a steady state. These findings must be verified in an independent dataset to ensure replicability and generalizability.

We examined the impact of schizophrenia on low-dimensional spatial dynamic states. Inferring from the dysconnectivity hypothesis (57), disturbances in behavior and psychopathology are expected to be associated with disruptions in the reconfiguration of system-wide brain functional integration. Our findings support this proposition by demonstrating significant alterations in the dynamics of spatial coupling in both men and women with schizophrenia.

In general, individuals with schizophrenia presented lower spFNC integration across all states and most networks. Specifically, the patterns of lower integration were more widespread in the MTRs and the right FPN (Figure 3). This is consistent with previous reports of global connectivity deficits in schizophrenia, with more prominent alterations in the frontal and temporal regions (58,59). We also found that individuals with schizophrenia presented, to a lesser extent, higher spFNC integration in specific pairs of networks, mainly involving the SUB, TEMP, MTRs, and CER (Figure 3). This is also consistent with previous reports of functional hyperconnectivity in individuals with schizophrenia (60–62).

While widespread disruption in networks' spatial coupling occurs across the whole brain and all dynamic states, the highly integrated, modular state 1 showed a great number of dysconnectivity patterns. The alterations observed in the pDMN/SN and right FPN/ATN spFNC in this state may be related to disturbances in cognition and psychopathology associated with psychosis (19,63). These findings are consistent with the triple-network model (63), suggesting that the abnormal striatal dopamine release may lead to disruptions in the dynamics among the DMN, SN, and FPN, thus potentially contributing to the misattribution of salience to irrelevant external stimuli and self-referential mental events.

Moreover, functional connectivity aberrations in the pDMN have repeatedly been shown to be involved with schizophrenia pathophysiology (64–66). Our results support and extend these findings by showing that disruptions in pDMN/SN spFNC were present in all 4 dynamic states (although this did not survive multiple comparison correction in state 3). Also, as hypothesized, we found a sex-by-diagnosis interaction effect for pDMN/SN spFNC in state 1, which could explain why some previous work found mixed results (65,67–69) or no alterations (70) in the DMN functional connectivity of individuals with schizophrenia. This pair also showed an association with the schizophrenia polygenic risk score, adding another layer of confirmation and suggesting a potential sex-specific psychosis neurobiological marker. However, the reproducibility of these results should be verified in an independent dataset.

Previous studies suggest that women diagnosed with schizophrenia tend to manifest more affective symptoms and often have overlapping diagnoses with affective psychosis (71,72). Negative symptoms tend to be more prevalent in men. Given the association between these symptoms and differences in cingulo-opercular and CER networks (73), our findings are consistent with the potential link between CER and SN and the observed sex differences.

Some spFNC pairs presented significant schizophrenia differences that were fleeting and temporally localized to only a few states (i.e., exhibited a state-like property), which contrasts with spFNC pairs where the schizophrenia effect was consistently present across all states (a trait-like property). The right FPN/ATN coupling exemplifies a state-like spFNC pair, whereas the TEMP/MTR-S pair is a notable trait-like example. Intriguingly, based on Neurosynth (https://www.neurosynth.org/) (74), the highest activation point for the TEMP is linked to semantic integration and language, while the peak activation for MTR-S is associated with speech production. Disruptions in language-related regions and networks in psychotic disorders are findings well-established in previous studies and may be linked to auditory verbal hallucinations (75–80). It should be noted that other pairs, such as pDMN/SN (with a diagnosis-by-sex interaction effect), MTR-S/SUB, MTR-S/CER, and SUB/CER, demonstrated a similar trait-like pattern, although the difference did not survive multiple comparison correction in all states (Figure 3A). Importantly, the schizophrenia changes in the MTR-S/SUB/CER support the cerebellar-thalamic-cortical dysconnectivity model of psychosis (81–83).

Another major finding is the spatial decoupling between the TEMP and MTR across all states, among which TEMP/MTR-P spFNC in state 2 is correlated with the schizophrenia polygenic risk score. Alterations in functional connectivity in temporal, somatosensory, and motor regions have previously been associated with schizophrenia (18), but to the best of our knowledge, this is the first study to show an association between those aberrations and genetic predisposition for schizophrenia. Individuals with schizophrenia often exhibit motor impairments from early stages, suggesting a genetic vulnerability contributing to neurodevelopmental disruptions (84,85). Temporal cortex dysfunction may also play a role in social cognition and theory of mind impairments in schizophrenia due to difficulties that individuals have detecting subtle emotional components of auditory inputs, which leads to reduced social interaction skills and marked deficiencies in psychosocial functioning (86). Additionally, the schizophrenia polygenic risk score reflects the overall genetic risk burden of 287 schizophrenia-related loci, for which a fine mapping revealed that 16 of the annotated genes had been implicated for credible causal nonsynonymous or untranslated region variation. The enrichment test has also pointed to a diverse set of synaptic proteins and suggested that multiple functional interactions of schizophrenia risk converge on synapses (54). While our findings link genetic risk for schizophrenia to TEMP/MTR, it would be intriguing to investigate whether this genetic predisposition could lead to synaptic alterations in these networks during neurodevelopment, thereby resulting in poor functional integration and the early emergence of neurological signs.

A significant breakthrough has been made regarding the significance of regions with weak functional connectivity (Figure 4). Our findings reveal that the distortion in spatial coupling was embedded in high-dimensional (voxel-level) space in brain regions with low contributions to the corresponding networks (Figure 4). For example, significant schizophrenia interaction and male diagnosis effects in the SN in state 1 were exclusively exhibited in regions with a low contribution to the SN. This observation is significant because current research often overlooks regions with small contributions during voxelwise analysis (i.e., uses a mask of regions

with high amplitude in spatial maps). This complements our recent finding (21) on the importance of time points with low contributions to capturing schizophrenia-related changes, calling for further investigation.

Taken together, our findings indicate that information about dynamic spatial dependence, which has been overlooked, holds immense potential to substantially impact the clinical landscape as it quantifies the continuous integration and segregation of brain networks. Particularly, it can advance our understanding of schizophrenia, a disorder that is often characterized by dysconnectivity and disruptions in system-wide functional integration.

Limitations and Future Directions

We confirmed the existence of these networks in both men and women, and our framework ensures comparability of findings between them. Nevertheless, there is a pressing need for new techniques that account for sex-specific differences when estimating brain networks.

Using spatially constrained ICA enables capturing brain networks from short data lengths (35), but its constraints limit comprehensive depiction of spatial dynamics and participant-specific features. Future research should develop optimized methods for more precise and thorough estimations of time-resolved participant-specific networks to improve our understanding of intricate spatial dynamics and individual variations in brain function. Furthermore, our study focused on dynamic spatial coupling, but a more comprehensive framework that includes temporal dynamics and static features is needed to characterize sex-common and sex-specific functional patterns of schizophrenia and their association with genetic risk factors.

In this study, we made choices based on existing knowledge from previous studies (49,51,52). However, the impact of different choices and the generalizability of clinical findings should be assessed in future studies, especially considering the inconsistency among previous schizophrenia-related findings. For example, future studies should investigate the impact of window lengths and spatial smoothing (35).

Factors, such as medication status and symptom severity, may influence the results and limit their applicability to other populations or specific subgroups. It is imperative to assess the replicability and generalizability of the findings in more homogeneous independent datasets with larger sample sizes, with a particular focus on medication use, symptom severity, substance use disorders, medical comorbidities, and years since symptom onset. While our post hoc analysis found no significant association between medication (chlorpromazine equivalence scores) and the 2 dynamic spFNC pairs with significant schizophrenia effects and genomic associations, evaluating the impact of different pharmacological treatments on schizophrenia-related changes in brain dynamics is critical. Additionally, future research should evaluate our findings in other cohorts, such as individuals with first-episode psychosis, individuals at high risk of psychosis, or first-degree relatives.

The correlation between the schizophrenia polygenic risk score and 2 specific spFNC aberrations suggests genetic influence on these changes and lends support to the neurodevelopmental hypothesis of schizophrenia, but the cross-sectional design precludes drawing causal inferences. Longitudinal studies with larger datasets are needed to elucidate the neurodevelopmental trajectory of schizophrenia.

Finally, the relevance of sex-specific findings should be interpreted while recognizing sex differences in the incidence and prevalence (higher in males) and the earlier onset of schizophrenia in men. Additionally, the limitations of statistical power underscore the need for larger sample sizes in future studies to validate these findings. Gender is another crucial factor that can influence our findings. Sex and gender differences in psychosis are the consequence of complex interactions between biological and psychosocial factors. It is essential to evaluate our findings in a dataset with both sex and gender information to discern between findings driven primarily by psychosocial or biological factors.

ACKNOWLEDGMENTS AND DISCLOSURES

This work was supported by the National Institutes of Health (Grant Nos. R01MH123610, R01EB020407, and R01MH118695 [to VDC] and Grant No. 5R01MH119251 [to AI]) and the National Science Foundation (Grant No 2112455 [to VDC]).

The authors report no biomedical financial interests or potential conflicts of interest.

ARTICLE INFORMATION

From the Tri-Institutional Center for Translational Research in Neuroimaging and Data Science, Atlanta, Georgia (AI, JC, NL, AF, ZF, OA, VDC); Department of Computer Science, Georgia State University, Atlanta, Georgia (AI); Department of Computational Science and Engineering, Georgia Institute of Technology, Atlanta, Georgia (NL, VDC); Maryland Psychiatric Research Center, Department of Psychiatry, School of Medicine, University of Maryland, Baltimore, Maryland (PK, BMA); Department of Psychiatry, University of California San Francisco, San Francisco, California (DHM); San Francisco Veteran Affairs Medical Center, San Francisco, California (DHM); Departments of Psychiatry and Neuroscience, Yale University School of Medicine, New Haven, Connecticut (GDP); Department of Psychiatry and Human Behavior, University of California Irvine, Irvine, California (FM, AP); Clinical Translational Neuroscience Laboratory, Department of Psychiatry and Human Behavior, University of California Irvine, Irvine, California (TGMvE); Department of Psychiatry and Behavioral Sciences, University of New Mexico, Albuquerque, New Mexico (JRB); Department of Child and Adolescent Psychiatry, Institute of Psychiatry and Mental Health, Hospital General Universitario Gregorio Marañón, Instituto de Investigación Sanitaria Gregorio Marañón, Madrid, Spain (CMDC, PA-C); Department of Physics and Astronomy, Georgia State University, Atlanta, Georgia (MD); and the Department of Computer Science and Electrical Engineering, University of Maryland, Baltimore County, Baltimore, Maryland (TA).

Address correspondence address to Armin Iraji, Ph.D., at armin.iraji@gmail.com, or Vince Calhoun, Ph.D., at vcalhoun@gsu.edu.

Received Jul 10, 2023; revised Nov 15, 2023; accepted Dec 1, 2023.

Supplementary material cited in this article is available online at https://doi.org/10.1016/j.biopsych.2023.12.002.

REFERENCES

1. Kadakia A, Catillon M, Fan Q, Williams GR, Marden JR, Anderson A, *et al.* (2022): The economic burden of schizophrenia in the United States. J Clin Psychiatry 83.
2. Green MF (2006): Cognitive impairment and functional outcome in schizophrenia and bipolar disorder. J Clin Psychiatry 67(suppl 9):3–8.
3. Tandon R, Nasrallah HA, Keshavan MS (2009): Schizophrenia, "just the facts" 4. Clinical features and conceptualization. Schizophr Res 110:1–23.

4. Paus T, Keshavan M, Giedd JN (2008): Why do many psychiatric disorders emerge during adolescence? Nat Rev Neurosci 9:947–957.
5. Dalsgaard S, Thorsteinsson E, Trabjerg BB, Schullehner J, Plana-Ripoll O, Brikell I, *et al.* (2020): Incidence rates and cumulative incidences of the full spectrum of diagnosed mental disorders in childhood and adolescence. JAMA Psychiatry 77:155–164.
6. Li R, Ma X, Wang G, Yang J, Wang C (2016): Why sex differences in schizophrenia? J Transl Neurosci (Beijing) 1:37–42.
7. Ochoa S, Usall J, Cobo J, Labad X, Kulkarni J (2012): Gender differences in schizophrenia and first-episode psychosis: A comprehensive literature review. Schizophr Res Treatment 2012:916198.
8. Mendrek A, Mancini-Marïe A (2016): Sex/gender differences in the brain and cognition in schizophrenia. Neurosci Biobehav Rev 67:57–78.
9. Goldstein JM, Cherkerzian S, Tsuang MT, Petryshen TL (2013): Sex differences in the genetic risk for schizophrenia: History of the evidence for sex-specific and sex-dependent effects. Am J Med Genet B Neuropsychiatr Genet 162B:698–710.
10. Frederikse M, Lu A, Aylward E, Barta P, Sharma T, Pearlson G (2000): Sex differences in inferior parietal lobule volume in schizophrenia. Am J Psychiatry 157:422–427.
11. Shifman S, Johannesson M, Bronstein M, Chen SX, Collier DA, Craddock NJ, *et al.* (2008): Genome-wide association identifies a common variant in the reelin gene that increases the risk of schizophrenia only in women. PLoS Genet 4:e28.
12. Zhang F, Chen Q, Ye T, Lipska BK, Straub RE, Vakkalanka R, *et al.* (2011): Evidence of sex-modulated association of ZNF804A with schizophrenia. Biol Psychiatry 69:914–917.
13. Blokland GAM, Grove J, Chen CY, Cotsapas C, Tobet S, Handa R, *et al.* (2022): Sex-dependent shared and nonshared genetic architecture across mood and psychotic disorders. Biol Psychiatry 91:102–117.
14. Koch E, Nyberg L, Lundquist A, Pudas S, Adolfsson R, Kauppi K (2021): Sex-specific effects of polygenic risk for schizophrenia on lifespan cognitive functioning in healthy individuals. Transl Psychiatry 11:520.
15. Buckholtz JW, Meyer-Lindenberg A (2012): Psychopathology and the human connectome: Toward a transdiagnostic model of risk for mental illness. Neuron 74:990–1004.
16. Friston KJ (2002): Dysfunctional connectivity in schizophrenia. World Psychiatry 1:66–71.
17. Calhoun VD, Sui J, Kiehl K, Turner J, Allen E, Pearlson G (2011): Exploring the psychosis functional connectome: Aberrant intrinsic networks in schizophrenia and bipolar disorder. Front Psychiatry 2:75.
18. Damaraju E, Allen EA, Belger A, Ford JM, McEwen S, Mathalon DH, *et al.* (2014): Dynamic functional connectivity analysis reveals transient states of dysconnectivity in schizophrenia. NeuroImage Clin 5:298–308.
19. Hare SM, Ford JM, Mathalon DH, Damaraju E, Bustillo J, Belger A, *et al.* (2019): Salience-default mode functional network connectivity linked to positive and negative symptoms of schizophrenia. Schizophr Bull 45:892–901.
20. Iraji A, Faghiri A, Fu Z, Rachakonda S, Kochunov P, Belger A, *et al.* (2022): Multi-spatial-scale dynamic interactions between functional sources reveal sex-specific changes in schizophrenia. Netw Neurosci 6:357–381.
21. Iraji A, Faghiri A, Fu Z, Kochunov P, Adhikari BM, Belger A, *et al.* (2022): Moving beyond the 'CAP' of the Iceberg: Intrinsic connectivity networks in fMRI are continuously engaging and overlapping. Neuroimage 251:119013.
22. Iraji A, Fu Z, Damaraju E, DeRamus TP, Lewis N, Bustillo JR, *et al.* (2019): Spatial dynamics within and between brain functional domains: A hierarchical approach to study time-varying brain function. Hum Brain Mapp 40:1969–1986.
23. Li S, Hu N, Zhang W, Tao B, Dai J, Gong Y, *et al.* (2019): Dysconnectivity of multiple brain networks in schizophrenia: A meta-analysis of resting-state functional connectivity. Front Psychiatry 10:482.
24. Dong D, Wang Y, Chang X, Luo C, Yao D (2018): Dysfunction of large-scale brain networks in schizophrenia: A meta-analysis of resting-state functional connectivity. Schizophr Bull 44:168–181.
25. Long Q, Bhinge S, Calhoun VD, Adali T (2021): Relationship between dynamic blood-oxygen-level-dependent activity and functional network connectivity: Characterization of schizophrenia subgroups. Brain Connect 11:430–446.
26. Pugliese V, de Filippis R, Aloi M, Rotella P, Carbone EA, Gaetano R, De Fazio P (2022): Aberrant salience correlates with psychotic dimensions in outpatients with schizophrenia spectrum disorders. Ann Gen Psychiatry 21:25.
27. Riecher-Rössler A, Butler S, Kulkarni J (2018): Sex and gender differences in schizophrenic psychoses-a critical review. Arch Womens Ment Health 21:627–648.
28. Carter B, Wootten J, Archie S, Terry AL, Anderson KK (2022): Sex and gender differences in symptoms of early psychosis: A systematic review and meta-analysis. Arch Womens Ment Health 25:679–691.
29. Long H, Fan M, Yang X, Guan Q, Huang Y, Xu X, *et al.* (2021): Sex-related difference in mental rotation performance is mediated by the special functional connectivity between the default mode and salience networks. Neuroscience 478:65–74.
30. Lawrence KE, Hernandez LM, Bowman HC, Padgaonkar NT, Fuster E, Jack A, *et al.* (2020): Sex differences in functional connectivity of the salience, default mode, and central executive networks in youth with ASD. Cereb Cortex 30:5107–5120.
31. Canitano R, Pallagrosi M (2017): Autism spectrum disorders and schizophrenia spectrum disorders: Excitation/inhibition imbalance and developmental trajectories. Front Psychiatry 8:69.
32. Iraji A, Miller R, Adali T, Calhoun VD (2020): Space: A missing piece of the dynamic puzzle. Trends Cogn Sci 24:135–149.
33. Allen EA, Erhardt EB, Damaraju E, Gruner W, Segall JM, Silva RF, *et al.* (2011): A baseline for the multivariate comparison of resting-state networks. Front Syst Neurosci 5:2.
34. Du Y, Fu Z, Sui J, Gao S, Xing Y, Lin D, *et al.* (2020): NeuroMark: An automated and adaptive ICA based pipeline to identify reproducible fMRI markers of brain disorders. NeuroImage Clin 28:102375.
35. Iraji A, Fu Z, Faghiri A, Duda M, Chen J, Rachakonda S, *et al.* (2023): Identifying canonical and replicable multi-scale intrinsic connectivity networks in 100k+ resting-state fMRI datasets. Hum Brain Mapp 44:5729–5748.
36. Schaefer A, Kong R, Gordon EM, Laumann TO, Zuo XN, Holmes AJ, *et al.* (2018): Local-global parcellation of the human cerebral cortex from intrinsic functional connectivity MRI. Cereb Cortex 28:3095–3114.
37. Craddock RC, James GA, Holtzheimer PE 3rd, Hu XP, Mayberg HS (2012): A whole brain fMRI atlas generated via spatially constrained spectral clustering. Hum Brain Mapp 33:1914–1928.
38. Yeo BT, Krienen FM, Sepulcre J, Sabuncu MR, Lashkari D, Hollinshead M, *et al.* (2011): The organization of the human cerebral cortex estimated by intrinsic functional connectivity. J Neurophysiol 106:1125–1165.
39. Iraji A, Deramus TP, Lewis N, Yaesoubi M, Stephen JM, Erhardt E, *et al.* (2019): The spatial chronnectome reveals a dynamic interplay between functional segregation and integration. Hum Brain Mapp 40:3058–3077.
40. Bhinge S, Long Q, Calhoun VD, Adali T (2019): Spatial dynamic functional connectivity analysis identifies distinctive biomarkers in schizophrenia. Front Neurosci 13:1006.
41. Boukhdhir A, Zhang Y, Mignotte M, Bellec P (2021): Unraveling reproducible dynamic states of individual brain functional parcellation. Netw Neurosci 5:28–55.
42. Aine CJ, Bockholt HJ, Bustillo JR, Cañive JM, Caprihan A, Gasparovic C, *et al.* (2017): Multimodal neuroimaging in schizophrenia: Description and dissemination. Neuroinformatics 15:343–364.
43. Adhikari BM, Hong LE, Sampath H, Chiappelli J, Jahanshad N, Thompson PM, *et al.* (2019): Functional network connectivity impairments and core cognitive deficits in schizophrenia. Hum Brain Mapp 40:4593–4605.

44. Power JD, Mitra A, Laumann TO, Snyder AZ, Schlaggar BL, Petersen SE (2014): Methods to detect, characterize, and remove motion artifact in resting state fMRI. Neuroimage 84:320–341.
45. Uddin LQ, Betzel RF, Cohen JR, Damoiseaux JS, De Brigard F, Eickhoff SB, *et al.* (2023): Controversies and progress on tandardization of large-scale brain network nomenclature. Netw Neurosci 7:864–905.
46. Calhoun VD, Adali T, Pearlson GD, Pekar JJ (2001): A method for making group inferences from functional MRI data using independent component analysis. Hum Brain Mapp 14:140–151.
47. Iraji A, Calhoun VD, Wiseman NM, Davoodi-Bojd E, Avanaki MRN, Haacke EM, Kou Z (2016): The connectivity domain: Analyzing resting state fMRI data using feature-based data-driven and model-based methods. Neuroimage 134:494–507.
48. Du Y, Fan Y (2013): Group information guided ICA for fMRI data analysis. Neuroimage 69:157–197.
49. Iraji A, Faghiri A, Lewis N, Fu Z, Rachakonda S, Calhoun VD (2021): Tools of the trade: Estimating time-varying connectivity patterns from fMRI data. Soc Cogn Affect Neurosci 16:849–874.
50. Du Y, Allen EA, He H, Sui J, Wu L, Calhoun VD (2016): Artifact removal in the context of group ICA: A comparison of single-subject and group approaches. Hum Brain Mapp 37:1005–1025.
51. Preti MG, Bolton TA, Van De Ville D (2017): The dynamic functional connectome: State-of-the-art and perspectives. NeuroImage 160: 41–54.
52. Allen EA, Damaraju E, Plis SM, Erhardt EB, Eichele T, Calhoun VD (2014): Tracking whole-brain connectivity dynamics in the resting state. Cereb Cortex 24:663–676.
53. Benjamini Y, Hochberg Y (1995): Controlling the false discovery rate: A practical and powerful approach to multiple testing. J R Stat Soc B (Methodol) 57:289–300.
54. Trubetskoy V, Pardiñas AF, Qi T, Panagiotaropoulou G, Awasthi S, Bigdeli TB, *et al.* (2022): Mapping genomic loci implicates genes and synaptic biology in schizophrenia. Nature 604:502–508.
55. Choi SW, Mak TSH, O'Reilly PF (2020): Tutorial: A guide to performing polygenic risk score analyses. Nat Protoc 15:2759–2772.
56. Ma S, Calhoun VD, Phlypo R, Adalı T (2014): Dynamic changes of spatial functional network connectivity in healthy individuals and schizophrenia patients using independent vector analysis. Neuroimage 90:196–206.
57. Friston K, Brown HR, Siemerkus J, Stephan KE (2016): The dysconnection hypothesis (2016). Schizophr Res 176:83–94.
58. Fornito A, Zalesky A, Pantelis C, Bullmore ET (2012): Schizophrenia, neuroimaging and connectomics. Neuroimage 62:2296–2314.
59. van den Heuvel MP, Fornito A (2014): Brain networks in schizophrenia. Neuropsychol Rev 24:32–48.
60. Liu H, Kaneko Y, Ouyang X, Li L, Hao Y, Chen EY, *et al.* (2012): Schizophrenic patients and their unaffected siblings share increased resting-state connectivity in the task-negative network but not its anticorrelated task-positive network. Schizophr Bull 38:285–294.
61. Walther S, Stegmayer K, Federspiel A, Bohlhalter S, Wiest R, Viher PV (2017): Aberrant hyperconnectivity in the motor system at rest is linked to motor abnormalities in schizophrenia spectrum disorders. Schizophr Bull 43:982–992.
62. Avram M, Brandl F, Bäuml J, Sorg C (2018): Cortico-thalamic hypo- and hyperconnectivity extend consistently to basal ganglia in schizophrenia. Neuropsychopharmacology 43:2239–2248.
63. Menon V, Palaniyappan L, Supekar K (2023): Integrative brain network and salience models of psychopathology and cognitive dysfunction in schizophrenia. Biol Psychiatry 94:108–120.
64. Hu ML, Zong XF, Mann JJ, Zheng JJ, Liao YH, Li ZC, *et al.* (2017): A review of the functional and anatomical default mode network in schizophrenia. Neurosci Bull 33:73–84.
65. Sheffield JM, Barch DM (2016): Cognition and resting-state functional connectivity in schizophrenia. Neurosci Biobehav Rev 61:108–120.
66. Meda SA, Ruaño G, Windemuth A, O'Neil K, Berwise C, Dunn SM, *et al.* (2014): Multivariate analysis reveals genetic associations of the resting default mode network in psychotic bipolar disorder and schizophrenia. Proc Natl Acad Sci USA 111:E2066–E2075.
67. Skudlarski P, Jagannathan K, Anderson K, Stevens MC, Calhoun VD, Skudlarska BA, Pearlson G (2010): Brain connectivity is not only lower but different in schizophrenia: A combined anatomical and functional approach. Biol Psychiatry 68:61–69.
68. Mingoia G, Wagner G, Langbein K, Maitra R, Smesny S, Dietzek M, *et al.* (2012): Default mode network activity in schizophrenia studied at resting state using probabilistic ICA. Schizophr Res 138:143–149.
69. Orliac F, Naveau M, Joliot M, Delcroix N, Razafimandimby A, Brazo P, *et al.* (2013): Links among resting-state default-mode network, salience network, and symptomatology in schizophrenia. Schizophr Res 148:74–80.
70. Wolf ND, Sambataro F, Vasic N, Frasch K, Schmid M, Schönfeldt-Lecuona C, *et al.* (2011): Dysconnectivity of multiple resting-state networks in patients with schizophrenia who have persistent auditory verbal hallucinations. J Psychiatry Neurosci 36:366–374.
71. Brand BA, de Boer JN, Dazzan P, Sommer IE (2022): Towards better care for women with schizophrenia-spectrum disorders. Lancet Psychiatry 9:330–336.
72. Sommer IE, Tiihonen J, van Mourik A, Tanskanen A, Taipale H (2020): The clinical course of schizophrenia in women and men-a nation-wide cohort study. npj Schizophr 6:12.
73. Mamah D, Barch DM, Repovš G (2013): Resting state functional connectivity of five neural networks in bipolar disorder and schizophrenia. J Affect Disord 150:601–609.
74. Yarkoni T, Poldrack RA, Nichols TE, Van Essen DC, Wager TD (2011): Large-scale automated synthesis of human functional neuroimaging data. Nat Methods 8:665–670.
75. DeLisi LE (2001): Speech disorder in schizophrenia: Review of the literature and exploration of its relation to the uniquely human capacity for language. Schizophr Bull 27:481–496.
76. Chang X, Collin G, Xi Y, Cui L, Scholtens LH, Sommer IE, *et al.* (2017): Resting-state functional connectivity in medication-naïve schizophrenia patients with and without auditory verbal hallucinations: A preliminary report. Schizophr Res 188:75–81.
77. Cui LB, Liu K, Li C, Wang LX, Guo F, Tian P, *et al.* (2016): Putamen-related regional and network functional deficits in first-episode schizophrenia with auditory verbal hallucinations. Schizophr Res 173:13–22.
78. Mueser KT, Bellack AS, Brady EU (1990): Hallucinations in schizophrenia. Acta Psychiatr Scand 82:26–29.
79. McCarthy-Jones S, Smailes D, Corvin A, Gill M, Morris DW, Dinan TG, *et al.* (2017): Occurrence and co-occurrence of hallucinations by modality in schizophrenia-spectrum disorders. Psychiatry Res 252:154–160.
80. Salisbury DF, Kohler J, Shenton ME, McCarley RW (2020): Deficit effect sizes and correlations of auditory event-related potentials at first hospitalization in the schizophrenia spectrum. Clin EEG Neurosci 51:198–206.
81. Woodward ND, Karbasforoushan H, Heckers S (2012): Thalamocortical dysconnectivity in schizophrenia. Am J Psychiatry 169:1092–1099.
82. Wei Y, Xue K, Yang M, Wang H, Chen J, Han S, *et al.* (2022): Aberrant cerebello-thalamo-cortical functional and effective connectivity in first-episode schizophrenia with auditory verbal hallucinations. Schizophr Bull 48:1336–1343.
83. Cao H, Ingvar M, Hultman CM, Cannon T (2019): Evidence for cerebello-thalamo-cortical hyperconnectivity as a heritable trait for schizophrenia. Transl Psychiatry 9:192.
84. Chan RC, Xu T, Heinrichs RW, Yu Y, Wang Y (2010): Neurological soft signs in schizophrenia: A meta-analysis. Schizophr Bull 36:1089–1104.
85. Bombin I, Arango C, Buchanan RW (2005): Significance and meaning of neurological signs in schizophrenia: Two decades later. Schizophr Bull 31:962–977.
86. Javitt DC, Sweet RA (2015): Auditory dysfunction in schizophrenia: Integrating clinical and basic features. Nat Rev Neurosci 16:535–550.